



Since January 2020 Elsevier has created a COVID-19 resource centre with free information in English and Mandarin on the novel coronavirus COVID-19. The COVID-19 resource centre is hosted on Elsevier Connect, the company's public news and information website.

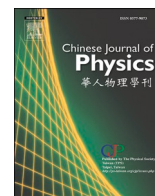
Elsevier hereby grants permission to make all its COVID-19-related research that is available on the COVID-19 resource centre - including this research content - immediately available in PubMed Central and other publicly funded repositories, such as the WHO COVID database with rights for unrestricted research re-use and analyses in any form or by any means with acknowledgement of the original source. These permissions are granted for free by Elsevier for as long as the COVID-19 resource centre remains active.



ELSEVIER

Contents lists available at ScienceDirect

Chinese Journal of Physics

journal homepage: [www.sciencedirect.com/journal/chinese-journal-of-physics](http://www.sciencedirect.com/journal/chinese-journal-of-physics)

# Leveraging elasticity of blood stenosis to detect the role of a non-Newtonian flow midst an arterial tube: Mazumdar and Keller models

A.M. Awad<sup>a</sup>, Kh.S. Mekheimer<sup>b</sup>, S.A. Elkilany<sup>a</sup>, A.Z. Zaher<sup>c,\*</sup>

<sup>a</sup> Mathematics Department, Faculty of Science, Kafrelsheikh University, Kafrelsheikh, Egypt

<sup>b</sup> Mathematical Department, Faculty of Science, Al-Azhar University, Nasr City 11884, Cairo, Egypt

<sup>c</sup> Engineering Mathematics and Physics Department, Faculty of Engineering - Shubra - Benha University, Egypt

## ARTICLE INFO

### Keywords:

Rubinow & Keller model  
Mazumdar model  
Herschel-Bulkley fluid  
stenosis arterial walls  
blood velocity

## ABSTRACT

Blood stenosis is considered one of the most serious risks which face humanity nowadays. In addition, it is also one of the most apparent symptoms of COVID (19) (Corona Virus). Consequently, this research is shedding light on studying the blood flow in case of having blood clots and artery elasticity in the presence of stenosis during studying the flow. Hematopoiesis requires a model of the yield stress fluid, and among the available yield stress fluid models for blood flow, the Herschel-Bulkley model is preferred (because Bingham, Power-law and Newtonian models are its special cases). Navier stokes equation is used to simulate this subject in a mathematical way. The elasticity on the stenosis arterial walls is simulated by Rubinow & Keller model [24] and Mazumdar model [25]. The results reveal exciting behaviors that, in turn, require adequate study of non-Newtonian fluid flow phenomena, especially the results showed that the increase in the parameters related to the elasticity of the walls facilitating the flow of blood through the stenosis area. In addition, a comparison between two elasticity models (Rubinow & Keller model and Mazumdar model) is considered. Further, for normal artery without stenosis, our results are the same as those obtained by Vajravelu et.al [22].

## 1. Introduction

**Atherosclerosis** is considered one of the most serious health problems facing man, which can be defined as the arterial lumen's blockage, which may occur partially or completely. Nowadays, the universe is badly suffering from an epidemic disease called Covid19 (Corona Virus), and as the *WHO*, (**World Health Organization**) has declared that the symptoms of this epidemic virus are blood stenosis, the chronic blockage pulmonary disease, and heart problems as coronary. Consequently, the blood flow's study, which is non-Newtonian fluids in the stenotic artery, is very significant. In recent times, Mekheimer and El Kot [1] made many studies related to the mathematical modeling of the flow's disorder of such fluids throughout anisotropic ally tapered flexible arteries compared with time variant stenosis's overlap. They were able to solve and examine their mathematical model for soft stenosis analytically. Riahi and his followers [2] had studied the artery flow of blood's problem in case of having interfering stenosis. This problem was studied mathematically, divided on three stages of intermittent blood flow through inflated arteries by Nadeem and Ijaz, [3]. In many of his

\* Corresponding author.

E-mail address: [abdullah.zaher@feng.bu.edu.eg](mailto:abdullah.zaher@feng.bu.edu.eg) (A.Z. Zaher).

<https://doi.org/10.1016/j.cjph.2022.04.006>

Received 23 March 2021; Received in revised form 23 March 2022; Accepted 10 April 2022

Available online 12 April 2022

0577-9073/© 2022 The Physical Society of the Republic of China (Taiwan). Published by Elsevier B.V. All rights reserved.

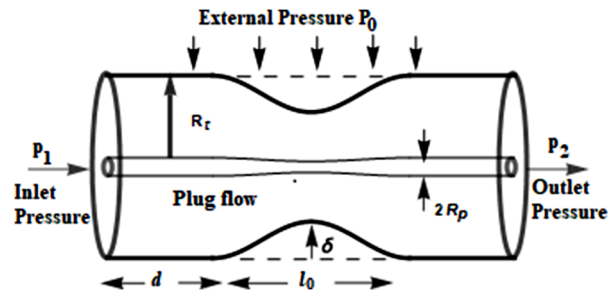


Figure 1. Geometry of the problem

research, Mekheimer et. al. [4–7] showed the various phases of analyzing blood flow in obstructive arteries. Herschel-Bulkley liquid is considered as a general sample of the non-Newtonian liquid, so the fluid pressure is related to pressure in general in a complicated non-linear style. That liquid sample also contains a yield stress factor and a force-law list and shows the shear-thinning attitudes and the stenosis parameter as well. If we want to get further information about the features of the flow of blood with the existence of a blood clot, we should use the Herschel-Bulkley equation because it contains many parameters. Besides, it can be reduced to different mathematical models or samples, and that can be done through taking suitable values of the coefficients. So, in order to reach more precise information about the flow of blood and decreased shear rates through limited arteries, man have to take into consideration the Herschel-Bulkley model. The reachable literary works on the Newtonian equation model show the Herschel-Bulkley fluid model with decrease shear standards [8–11] in different physical conditions. Jie WU and others [12] illustrate a tumor blood perfusion 3D numerical study and oxygen transport during vascular normalization. Ellahi and others [13] studied Blood flow of Jeffrey fluid in a catheterized tapered artery with the suspension of nanoparticles. In the last decades, blood flow was studied by Mirza and his colleagues [14] through Magnetohydrodynamic approach of non-Newtonian blood flow with magnetic particles in stenosed artery. Bhatti and colleagues [15] developed a mathematical model to more accurately simulate electromagnetic flow to show the effects of a clot on peristaltic motion during a Prandtl fluid through an irregular loop. Tripathi and his colleagues [16] explained several effects on Cu-CuO nanofluids, including thermal and electromagnetic field inside microvasculature. Rana and others [17] used the Oldroyd model with mixed convection on a flexible surface with microscopic microorganisms under the influence of suction/injection. In addition, Ellahi and others [18] studied the flow of blood via the composite stenosis of a non-Newtonian Micropolar fluid. Bhatti and Abdelsalam [19] demonstrated the peristaltic motion of carreau fluid in a symmetric channel under the influence of an applied and induced magnetic field and combined Tantalum (Ta) and Gold (Au) particles. The goal of Asmaa and others [20] was to study a mathematical model with numerical simulation through the use of a non-Newtonian fluid for Casson blood flow in the heart valve. Waqas and others [21] have investigated the phenomenon of biological fluctuation in 3D nanofluids flow Maxwell with several properties. On the other hand, the introduction of the elastic property of tube wall makes modeling and simulation more exciting for understanding many infusion problems in medicine, biology, and biomedical technology. The elastic property of the material is its ability to resist deforming force, it retains its original shape immediately after the force is removed which is quite natural. Elasticity occupies a significant role in the blood's flow inside the arteries, as it is called an elastic artery, for example, the arteries near the heart. It expands during the work of the heart, "Systole," which makes it suitable for transportation and absorbs the excess amount of blood that the following arteries cannot pass it is completely at the time of the work of the heart. While contracts at the time of the heart muscle "diastole" and thus is emptied of blood content through pressure because of the liquid it contains and returns to its original form. Hence the phenomenon of continuous blood flow and protection of the peripheral arteries from the high differential pressure between the working and resting periods of the heart. In addition, the elasticity of the arteries helps in the blood's flow with the existence of stenosis since it helps in the diagonal expansion of the arteries. Herschel-Bulkley fluid flow was also examined and studied in the elastic tube with a catheter by Vajravelu et al [22]. On the other hand, the presence of the elasticity of the tube wall makes the model relevant in terms of solution. The vascular system also consists of a complex formation of branched flexible tubes. From the literature that focuses on the problem in general. Young [23] began to appreciate the importance of elasticity to the heartbeat. Fung [24] considered Poiseuille's flow, and found that the tube radius could be determined by the balance between the transient pressure (i. e. the difference between the inside and outside pressure) and the tension in the tube wall. Sochi [25] examined the flow of Newtonian fluids and the power law in flexible tubes, taking into account the lubrication approximation theory. According to the above, the elastic tubes were not used on a wide scale. So, a little work was done by them with the existence of stenosis. As a result, we study in this research the flow of Herschel-Bulkley liquid via a flexible pipe with a catheter and a narrow (thrombosis). In this research, we are able to solve the equations through two elasticity models: Rubinow & Keller model and Mazumdar model, and we compare and contrast the solutions of the two models in the output figures appearing to get a precise solution to the incompressible flow of blood through having the stenosis. First, the problem normed and then facilitated by using non-dimensional variables. After this facilitated solution, equations for speed, flow, and pressure gradient are found and the results are debated through graphics of different substantial framework of the problem. In the present paper, the 1st Section is an introduction, while Section 2 includes the mathematical formula, Section 3 includes the appropriate solutions to the problems, in Section 4<sup>th</sup> includes Validation, while the 5<sup>th</sup> Section incorporates the discussion and the outcomes, and the 6<sup>th</sup> Section summarizes the fundamental points.

## 2. Essential equations as well as the mathematical conceptualization

Think about the flow of a laminar incompressible Herschel-Bulkley fluid in an elastic tube (look at Figure 1) of radius  $R(z)$  and length  $L$ . An elasticity in a stenosis arterial tube is simulated by Rubinow & Keller model and Mazumdar model. The blood is sculptured as a non-Newtonian Herschel-Bulkley liquid and the flow is axisymmetric. The pivotal geometry facilitates the selection of the cylindrical correlate system  $(r, \varphi, z)$ , in which  $r$  and  $z$  indicate the radial and the axial correlate and  $\varphi$  is the azimuthal angle.

The fundamental equations that govern the fluid are:

$$\text{div } V = 0 \tag{1}$$

$$\text{div } \sigma + \rho f = \rho \frac{dV}{dt} \tag{2}$$

$V$  stands for velocity,  $f$  symbolizes the body force per unit mass,  $\rho$  stands for the density,  $\frac{d}{dt}$  stands for the material derivative, and  $\sigma$  symbolizes the Cauchy stress recognized by

$$\sigma = -Pl + T \tag{3}$$

$$T = 2\mu D + S \tag{4}$$

$$S = 2\eta D \tag{5}$$

$D$  is considered as symmetric part of the velocity gradient, and it can be defined by  $D = \frac{1}{2}[L + L^T]$  and  $L = \text{grad } V$ . As well,  $-Pl$  indicates the unspecified section of the stress because of the hindrance of incompressibility;  $\mu$  as well as  $\eta$  are consistence. The stenosis's geometry is supposed to be proved in the arterial section which, in turn, is shown as [1]:

$$\bar{R}(\bar{z}) = \bar{R}_r - \frac{\delta}{2} \left[ 1 + \cos \frac{2\pi}{l_0} \left( \bar{z} - d - \frac{l_0}{2} \right) \right]; d \leq \bar{z} \leq d + l_0 \tag{6}$$

$$\bar{R}(\bar{z}) = \bar{R}_r; \text{ other wise} \tag{7}$$

Here,  $\bar{R} \approx \bar{R}(\bar{z})$  and  $\bar{R}_r$  are the parameter of the artery including or excluding stenosis, is severally,  $l_0$  indicates the stretch of the stenosis,  $d$  refers to the location,  $\delta$  is the highest degree of protection (climax) of the stenosis at  $\bar{z} = d + \frac{l_0}{2}$ . The momentum equation which rules the motion is [22]:

$$\frac{\partial \bar{u}}{\partial \bar{r}} + \frac{\bar{u}}{\bar{r}} + \frac{\partial \bar{w}}{\partial \bar{z}} = 0 \tag{8a}$$

$$\rho \left( \frac{\partial}{\partial t} + \bar{u} \frac{\partial}{\partial \bar{r}} + \bar{w} \frac{\partial}{\partial \bar{z}} \right) \bar{u} = -\frac{\partial \bar{P}}{\partial \bar{r}} + \frac{1}{\bar{r}} \frac{\partial \bar{r}}{\partial \bar{r}} \bar{\tau}_{rr} + \frac{\partial \bar{\tau}_{rz}}{\partial \bar{z}} \tag{8b}$$

$$\rho \left( \frac{\partial}{\partial t} + \bar{u} \frac{\partial}{\partial \bar{r}} + \bar{w} \frac{\partial}{\partial \bar{z}} \right) \bar{w} = -\frac{\partial \bar{P}}{\partial \bar{z}} + \frac{1}{\bar{r}} \frac{\partial \bar{r}}{\partial \bar{r}} \bar{\tau}_{rz} + \frac{\partial \bar{\tau}_{zz}}{\partial \bar{z}} \tag{8c}$$

In which  $\bar{\tau}_{rz}$  is the Herschel-Bulkley's shear stress of liquid and can be shown through:

$$\bar{\tau}_{rz} = \mu \left( -\frac{\partial \bar{w}}{\partial \bar{r}} \right)^n + \bar{\tau}_p, \bar{\tau}_{rz} > \bar{\tau}_p, \tag{9}$$

$$\frac{\partial \bar{w}}{\partial \bar{r}} = 0, \bar{\tau}_{rz} < \bar{\tau}_p \tag{10}$$

Moving forward,  $w$  symbolizes the pivotal speed,  $p$  indicates the pressure (physical force),  $\bar{\tau}_p$  is presented as the yield stress. We should take into consideration that if yield stress is higher than the shear stress, i.e.,  $\bar{\tau}_{rz} < \bar{\tau}_p$  we will have a fundamental area which, in turn, surges and works as a stopper and equation (7) concurs to the disappearing speed grade in that area. Even so, the model of fluid we are relying on here is as shown above for  $\bar{\tau}_{rz} > \bar{\tau}_p$ . the boundary conditions are as follows [22]:

$$\bar{\tau}_{rz} \text{ is finite at } \bar{r} = 0, \tag{11}$$

$$\bar{w} = 0 \text{ at } \bar{r} = \bar{R}(\bar{z}) \tag{12}$$

## 3. Problem's resolution

To solve equations (8) as well as (9) according to the boundary conditions (11) and (12), the following non-dimensional quantities should be used:

$$\begin{aligned}
 r &= \frac{\bar{r}}{R_0}, t = \frac{u_0 \bar{t}}{l_0}, R_p = \frac{\bar{R}_p}{R_0}, R_t = \frac{\bar{R}_t}{R_0}, R(z) = \frac{\bar{R}(z)}{R_0}, z = \frac{\bar{z}}{l_0}, u = \frac{l_0 \bar{u}}{U \delta}, w = \frac{\bar{w}}{U}, \delta = \frac{\bar{\delta}}{R_0}, \\
 P &= \frac{R_0^{n+1}}{\mu U^n} \bar{P}, \tau_p = \frac{\bar{\tau}_p}{\mu \left(\frac{U}{R_0}\right)^n}, \tau_{rz} = \frac{\bar{\tau}_{rz}}{\mu \left(\frac{U}{R_0}\right)^n}, \tau_{rr} = \frac{\bar{\tau}_{rr}}{\mu \left(\frac{U}{R_0}\right)^n}, \tau_{zz} = \frac{\bar{\tau}_{zz}}{\mu \left(\frac{U}{R_0}\right)^n}
 \end{aligned}
 \tag{13}$$

As a consequence,  $P = \frac{\partial p}{\partial z}$ ,  $R_0$  is the tube's radius at inlet,  $U$  indicates the average speed, and  $R_p$  points to the plug flow radius's area. The following assumptions are considered to deal with a mild stenosis case  $\delta = \frac{\bar{\delta}}{R_0} \ll 1$ , we find that

$$\frac{1}{r} \frac{\partial}{\partial r} (r \tau_{rz}) = P
 \tag{14}$$

The following shows the non-dimensional the boundary conditions:

$$\tau_{rz} \text{ is finite at } r = 0,
 \tag{15a}$$

$$w = 0 \text{ at } r = R(z).
 \tag{15b}$$

$$R(z) = R_t - \frac{\delta}{2} \left[ 1 + \cos 2\pi \left( z - \varepsilon - \frac{1}{2} \right) \right]; \varepsilon \leq z \leq \varepsilon + 1,
 \tag{16a}$$

$$R(z) = R_t; \text{ other wise.}
 \tag{16b}$$

Where  $\varepsilon = \frac{d}{l_0}$ , by finding a solution to [equation \(14\)](#) with conditions (15), the velocity field is obtained as:

$$w = \frac{2}{P \left(\frac{1}{n} + 1\right)} \left[ \left(\frac{P}{2} R - \tau_p\right)^{\frac{1}{n} + 1} - \left(\frac{P}{2} r - \tau_p\right)^{\frac{1}{n} + 1} \right]
 \tag{17}$$

If the boundary conditions (11) are used, which is the higher limit of the plug flow area [i.e., the area between  $r = 0$  and  $r = R_p$  and for which ( $\tau_{rz} < \tau_p$ )] is gained as

$$R_p = \frac{2\tau_p}{P}
 \tag{18}$$

In addition, if we use the condition  $\tau_{rz} = \tau_R$  at  $r = R$  we can get:

$$P = \frac{2\tau_R}{R}
 \tag{19}$$

Consequently,

$$\frac{R_p}{R} = \frac{\tau_p}{\tau_R} = \tau, \quad 0 < \tau < 1.
 \tag{20}$$

We gain the plug flow speed in case of using the relevance (20) and getting  $r = R_p$  in sum (17),

$$w_p = \left(\frac{P}{2}\right)^{\frac{1}{n}} \frac{(R)^{\frac{1}{n} + 1}}{\left(\frac{1}{n} + 1\right)} (1 - \tau)^{\frac{1}{n} + 1} \text{ for } 0 \leq r \leq R_p.
 \tag{21}$$

Through any cross-section, and the flow rate  $Q$  can be obtained through:

$$Q = 2 \left[ \int_0^{R_p} w_p r \, dr + \int_{R_p}^R w r \, dr \right] = \frac{(1 - \tau)^{\frac{1}{n} + 1}}{(2)^{\frac{1}{n}} \left(\frac{1}{n} + 1\right)} \left[ 1 - \frac{2(1 - \tau) \left(\tau + \frac{1}{n} + 2\right)}{\left(\frac{1}{n} + 2\right) \left(\frac{1}{n} + 3\right)} \right] (R)^{\frac{1}{n} + 3} (P)^{\frac{1}{n}}.
 \tag{22}$$

According to the previous [equation \(22\)](#), it shows the capacity fluidity for a conduit of different radius  $R$ . Depending on the fact that the variation happens because of the flexibility of the conduit wall, the Poiseuille's law can be assumed for Herschel-Bulkley liquid stream in a flexible conduit with existence stenosis and the outcomes can be discussed in the coming section.

### 3.1. Determination of the theoretical fluidity

Now, the flow rate  $Q$  can be calculated theoretically according to a non-compressible Herschel-Bulkley liquid of viscosity  $\mu$  in a flexible conduit (look at [Figure 1](#)) of radius  $R(z)$  as well as extension  $L$ . The liquid goes into the conduit because of the pressure  $P_1$  and it goes out with less pressure  $P_2$ , but the pressure that is goes outside the conduit is  $P_0$ . If we assume that  $z$  points at the distance along the conduit from the inlet end, hence, the pressure  $P(z)$  in the liquid at  $z$  reduces from  $P(0) = P_1$  to  $p(L) = P_2$ . As a result of the pressure variation  $P(z) - P_0$ , between the internal and the external parts of the conduit, the conduit may become larger or shrinks, besides, we

may have deformation in its cross-shape section and that may be because of the flexible validity of the wall. So, the conduction  $\sigma_1$  of the conduit at  $z$  will be relying on the pressure variation. We put into consideration  $\sigma_1 = \sigma_1[P(z) - P_0]$  as a familiar sum of  $P(z) - P_0$ . We can suppose that this conduction is similar to a uniform conduit which has the same cross section as what we can find at  $z$ . It's supposed that the  $Q$  is interconnected to the pressure grade throw the relation:

$$Q = \sigma_1(P - P_0) \left( -\frac{\partial P}{\partial z} \right)^{\frac{1}{n}}, \tag{23}$$

Where

$$\sigma_1(P - P_0) = FR^{\frac{1}{n}+3}$$

And

$$F = \frac{(1 - \tau)^{\frac{1}{n}+1}}{(2)^{\frac{1}{n}} \left( \frac{1}{n} + 1 \right)} \left[ 1 - \frac{2(1 - \tau) \left( \tau + \frac{1}{n} + 2 \right)}{\left( \frac{1}{n} + 2 \right) \left( \frac{1}{n} + 3 \right)} \right]$$

If we take into consideration the flexible feature as well as the meandrous motion, we will have:

$$\sigma_1(P - P_0) = F(R + R')^{\frac{1}{n}+3} \tag{24}$$

Where is the change in the radius of the tube due to elasticity Here, when  $n = 1$  and  $\tau = 0$ , [equation \(23\)](#) decreases to the presumption of Keller and Rubinow [27] as a Newtonian-liquid flow in a flexible conduit and correlating [equation \(23\)](#) liable to  $z$  from  $z = 0$  as well as using the internal circumference  $P(0) = P_1$ , the following will be obtained:

$$Q^n z = \int_{P(z)-P_0}^{P_1-P_0} (\sigma_1(P'))^n dP' \tag{25}$$

The  $P' = P(z) - P_0$ . This equation denotes  $P(z)$  in an impeded way in the absence of  $Q$  and  $z$ . In order to find  $Q$ , put  $z = 1$  and  $P(1) = P_2$  in [equation \(25\)](#) so that we can get:

$$Q^n = \int_{P(1)-P_0}^{P_1-P_0} (\sigma_1(P'))^n dP' \tag{26}$$

Related to current case (circular cross section), the radius  $R'$  is shown as a function of  $P - P_0$ , that is  $R' = R'(P - P_0)$ . We can also write [equation \(26\)](#) as:

$$Q^n = F^n \int_{P_2-P_0}^{P_1-P_0} (R + R')^{3n+1} dP' \tag{27}$$

We can also find a solution to [equation \(27\)](#) in case of knowing the structure of the function  $R'(P - P_0)$ . When the hoop stress or tension  $T(R')$  in the tube wall is recognized as a function of  $R'$ , in this case  $R'(P - P_0)$  can be specified by the equilibrium condition as follows:

$$\frac{T(R')}{R'} = (P - P_0). \tag{28}$$

### 3.2. The Flow's Application through a stenotic Artery

By considering the wall elasticity of blood artery with stenosis and using the pressure difference  $P(z) - P_0$ , therefore the conduct  $\sigma_1$  is assumed to be the same as that of a uniform artery tube having the same cross section  $z$ .

There are two different methods through which we can recognize the arterial flow:

#### 3.2.1. Rubinow and Keller's methods

The consistent relationship which can be found between the volume and pressure of a 4 cm segment of the external iliac of a human artery and its transformation into a tension-to-length curve were determined by Burton and Roach [26]. They used a method of the least squares (Rubinow and Keller [27]) the result:

$$T(R') = t_1(R' - 1) + t_2(R' - 1)^5, \tag{29}$$

Here,  $t_1 = 13$  and  $t_2 = 300$ .

**Table 1**

Comparison between the results of the flux Q with the radius of the tube R(z) extracted by the Rubinow and Keller model for  $\delta = 0$  and  $\delta = 0.1$ .

$\delta = 0$ [22]							
$n=1, \tau=0$		$n=1, \tau=0.2$		$n=3, \tau=0$		$n=3, \tau=0.2$	
Q	R(z)	Q	R(z)	Q	R(z)	Q	R(z)
0.075	0	0.055	0	$1.886 \times 10^{-7}$	0	$1.33 \times 10^{-7}$	0
0.576	0.1	0.423	0.1	0.00002	0.1	0.000012	0.1
2.26	0.2	1.658	0.2	0.0005	0.2	0.00033	0.2
6.284	0.3	4.613	0.3	0.0056	0.3	0.0039	0.3
14.21	0.4	10.43	0.4	0.04	0.4	0.028	0.4
$\delta \neq 0$ (our results)							
$n=1, \tau=0$		$n=1, \tau=0.2$		$n=3, \tau=0$		$n=3, \tau=0.2$	
Q	R(z)	Q	R(z)	Q	R(z)	Q	R(z)
0.0019	0	0.0014	0	$8.05 \times 10^{-11}$	0	$5.66 \times 10^{-11}$	0
0.075	0.1	0.055	0.1	$1.89 \times 10^{-7}$	0.1	$1.33 \times 10^{-7}$	0.1
0.576	0.2	0.423	0.2	0.00002	0.2	.000013	0.2
2.25	0.3	1.658	0.3	0.0005	0.3	0.00033	0.3
6.284	0.4	4.612	0.4	0.0065	0.4	0.0039	0.4

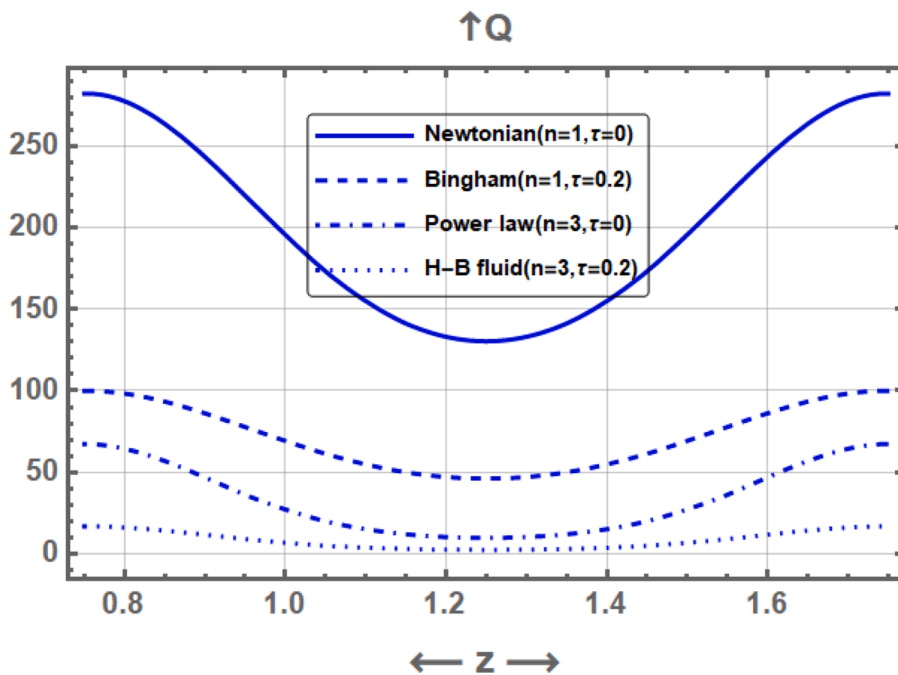


**Figure 2.** Keller model (variation of flux Q with z for different fluids with a change in power law-index (n) and yield stress ( $\tau$ )).

When we replace (29) in (28) obtaining:

$$dP' = \left[ \frac{t_1}{R'^2} + t_2 \left( 4R'^3 - 15R'^2 + 20R' - 10 + \frac{1}{R'^2} \right) \right] dR', \tag{30}$$

Using equation (30) and (27) we can write as them follows:

$$Q^n = F^n \int_{P_2-P_0}^{P_1-P_0} (R + R')^{3n+1} \left[ \frac{t_1}{R'^2} + t_2 \left( 4R'^3 - 15R'^2 + 20R' - 10 + \frac{1}{R'^2} \right) \right] dR' \tag{31}$$

The equation (31) decreases to the matching consequences of Rubinow and Keller [27] as related to the flow of Newtonian fluid (hence,  $n = 1, \tau = 0$ ) in a flexible conduit can be observed.

### 3.2.2. Mazumdar’s method

If we follow Mazumdar [28], the relationship of tension can be expressed as follows:

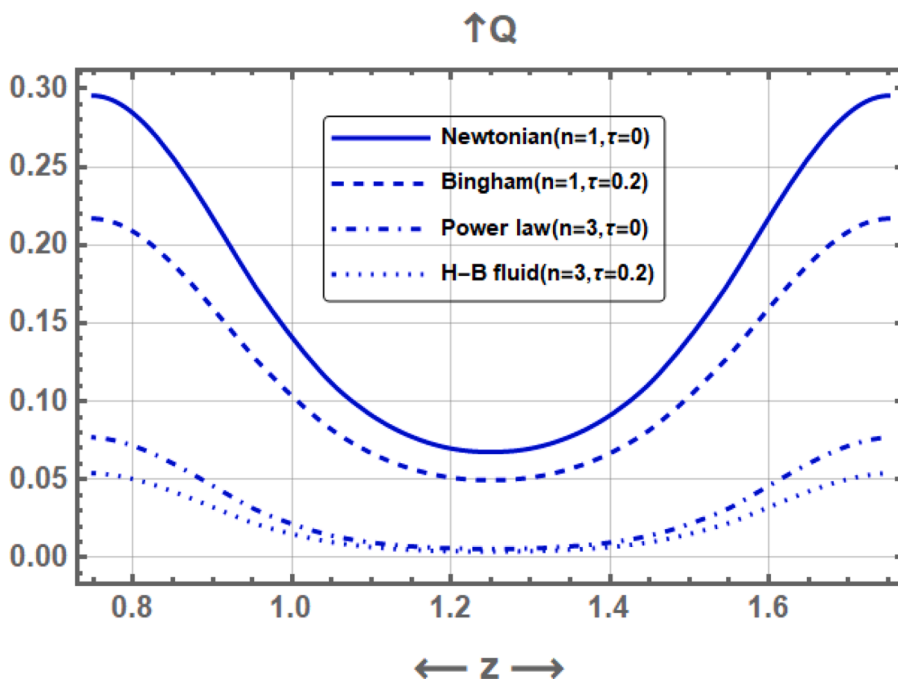


Figure 3. Mazumdar model (variation of flux  $Q$  with  $z$  for different fluids with a change in power law-index ( $n$ ) and yield stress ( $\tau$ )).

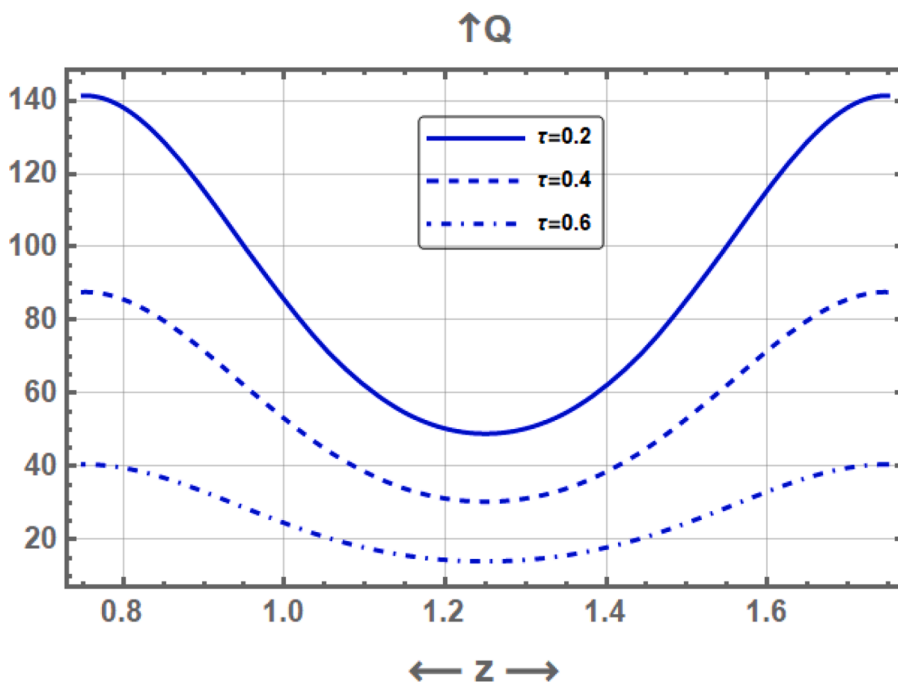


Figure 4. Keller model (variation of flux  $Q$  with  $z$  for different values of yield stress ( $\tau$ )).

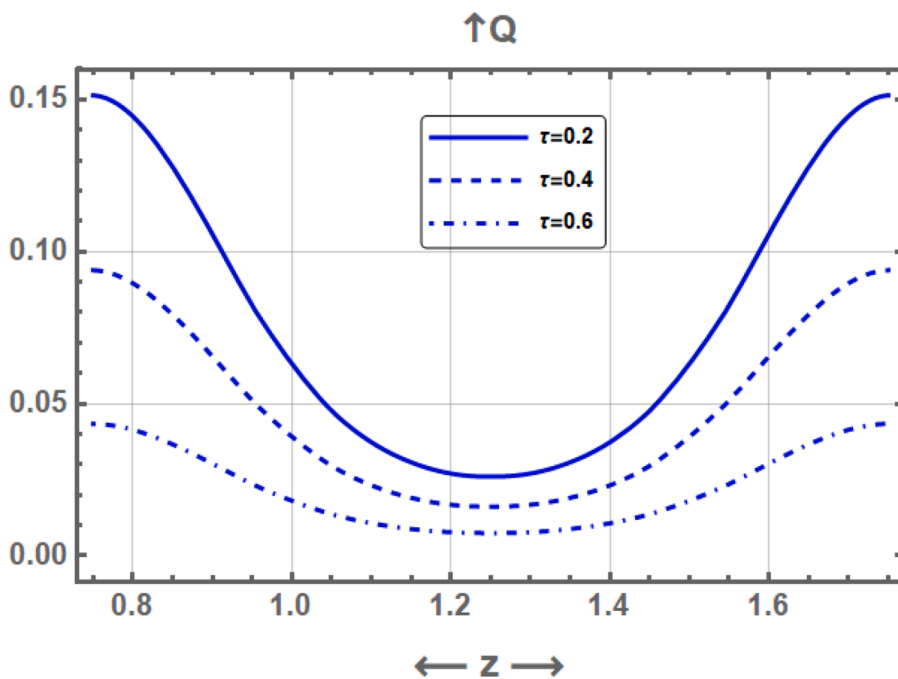


Figure 5. Mazumdar model (variation of flux  $Q$  with  $z$  for different values of yield stress ( $\tau$ )).

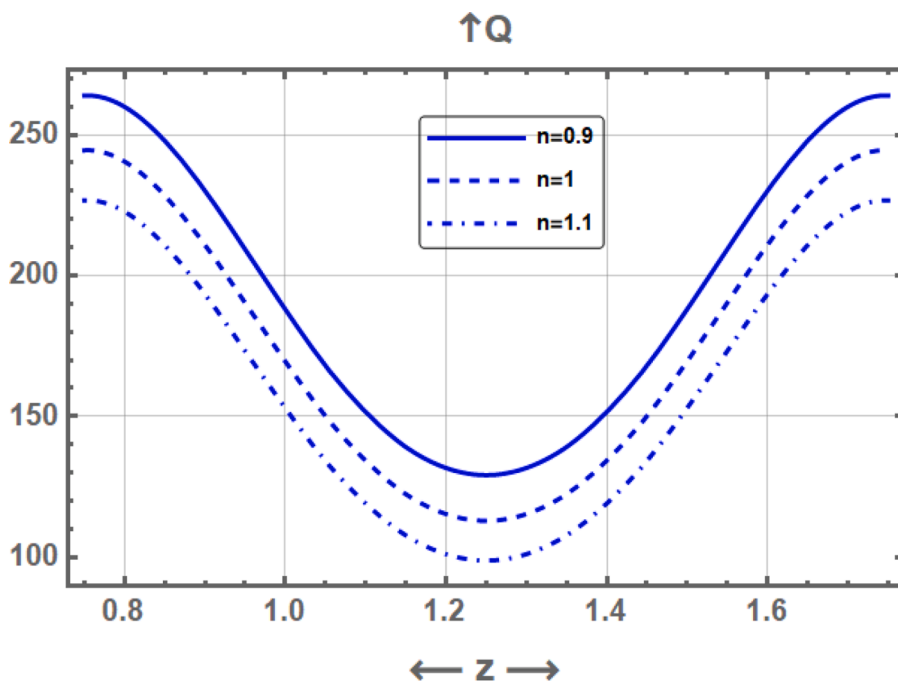


Figure 6. Keller model (variation of flux  $Q$  with  $z$  for different values of power law-index ( $n$ )).

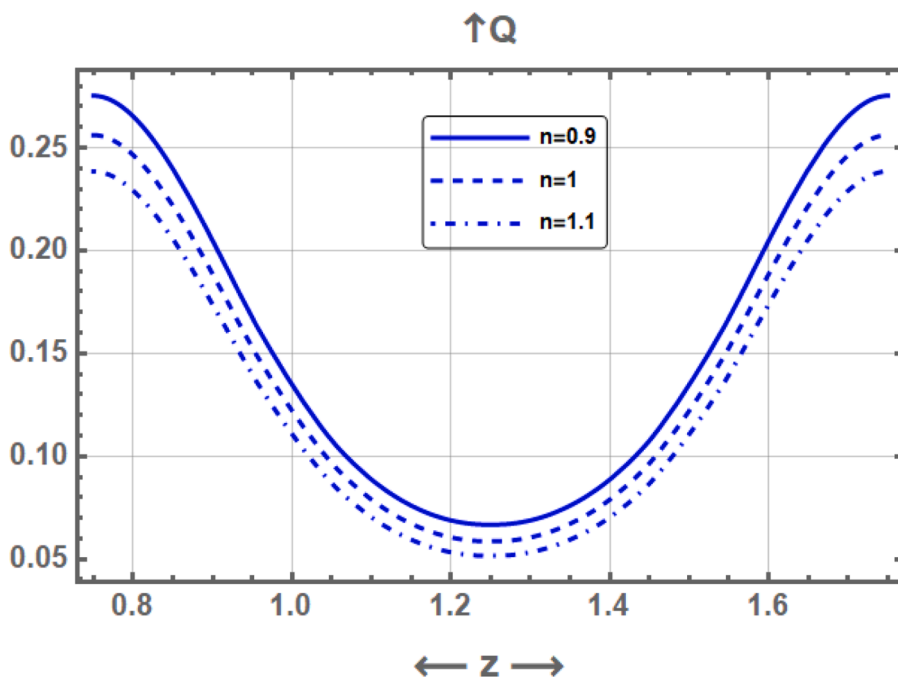


Figure 7. Mazumdar model (variation of flux  $Q$  with  $z$  for different values of power law-index ( $n$ )).

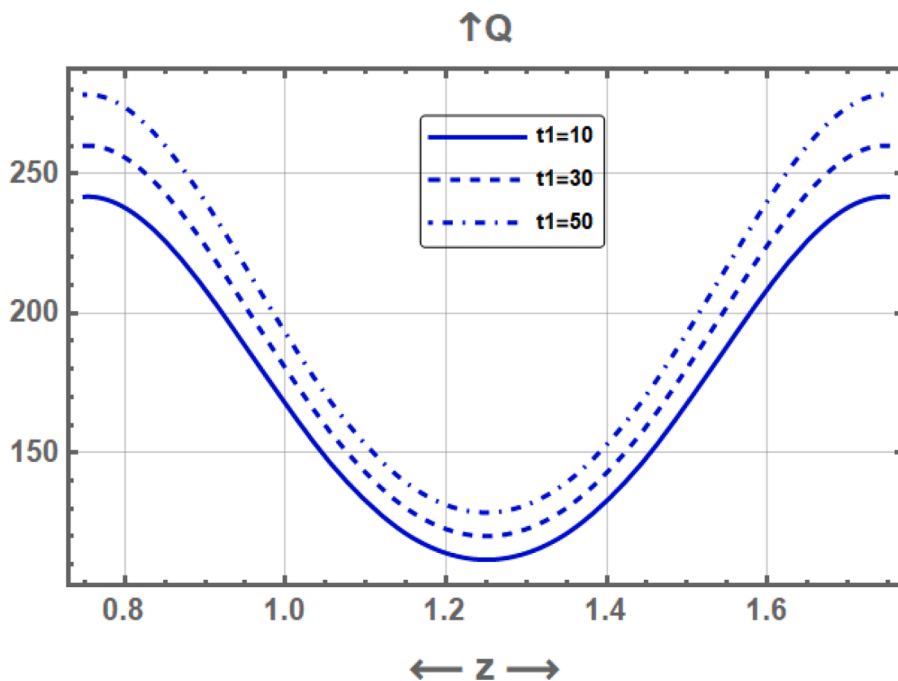


Figure 8. Keller model (variation of flux  $Q$  with  $z$  for different values of elastic parameter ( $t_1$ )).

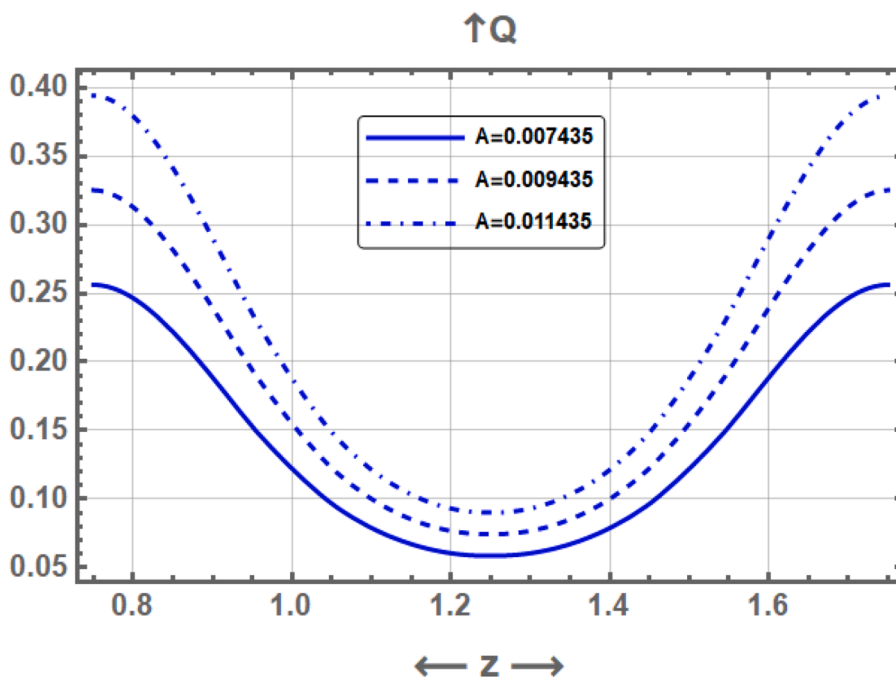


Figure 9. Mazumdar model (variation of flux  $Q$  with  $z$  for different values of elastic parameter ( $A$ )).

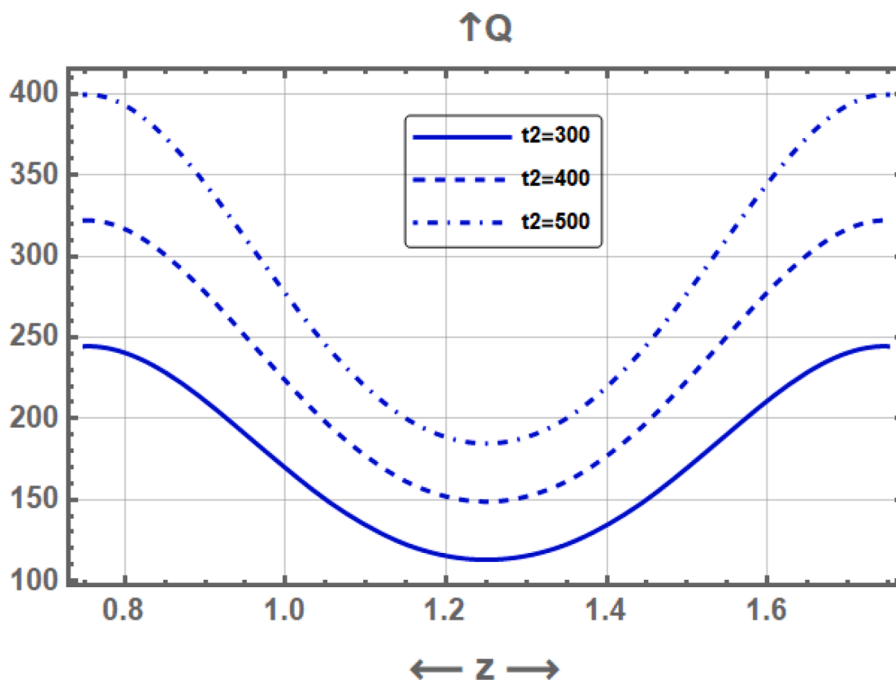


Figure 10. Keller model (variation of flux  $Q$  with  $z$  for different values of elastic parameter ( $t_2$ )).

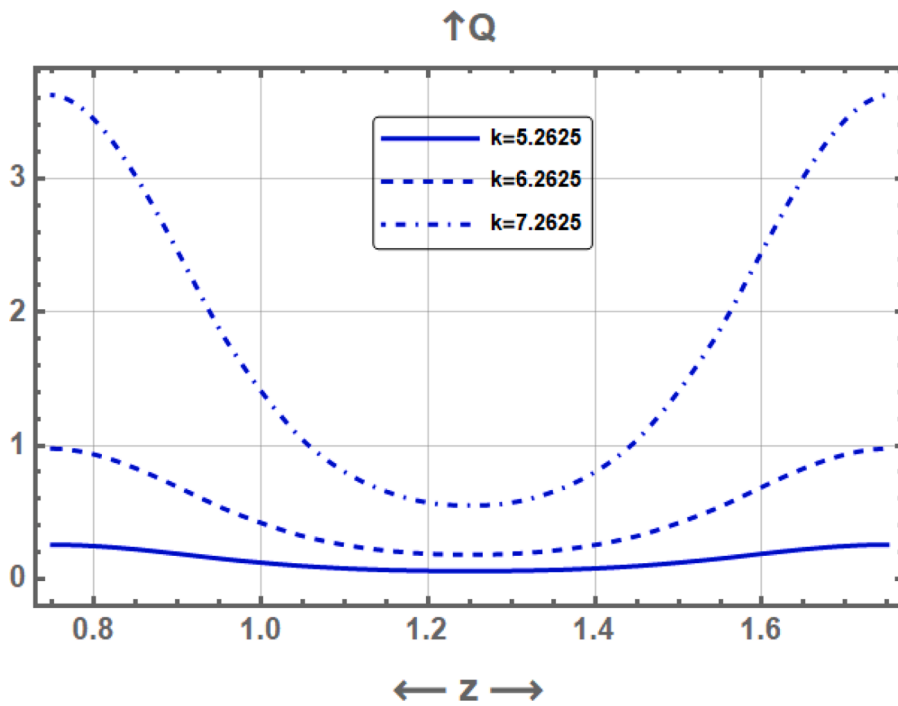


Figure 11. Mazumdar model (variation of flux  $Q$  with  $z$  for different values of elastic parameter ( $k$ )).

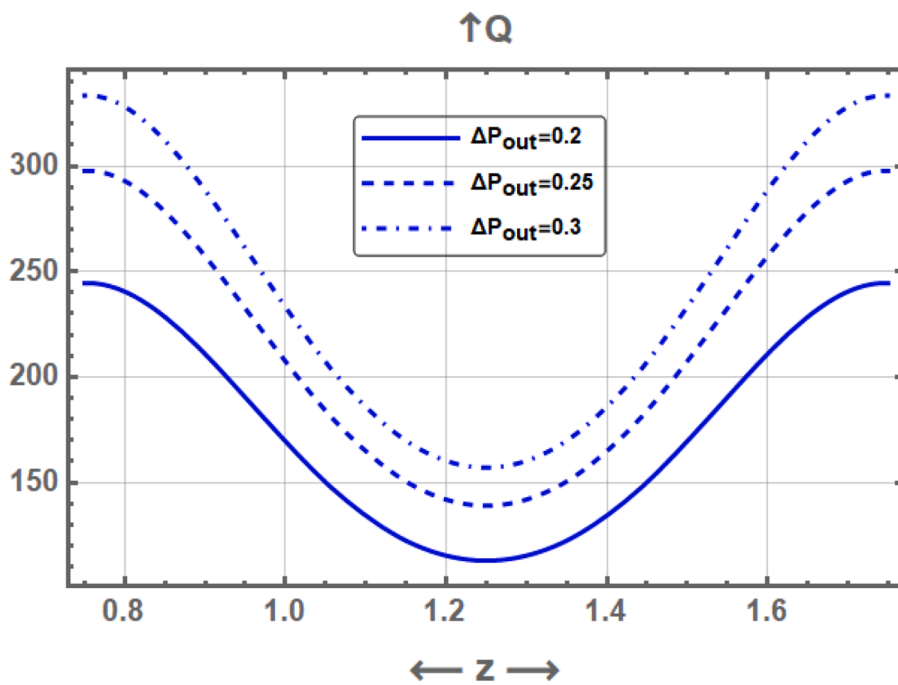


Figure 12. Keller model (variation of flux  $Q$  with  $z$  for different values of  $\Delta P_{out}$ ).

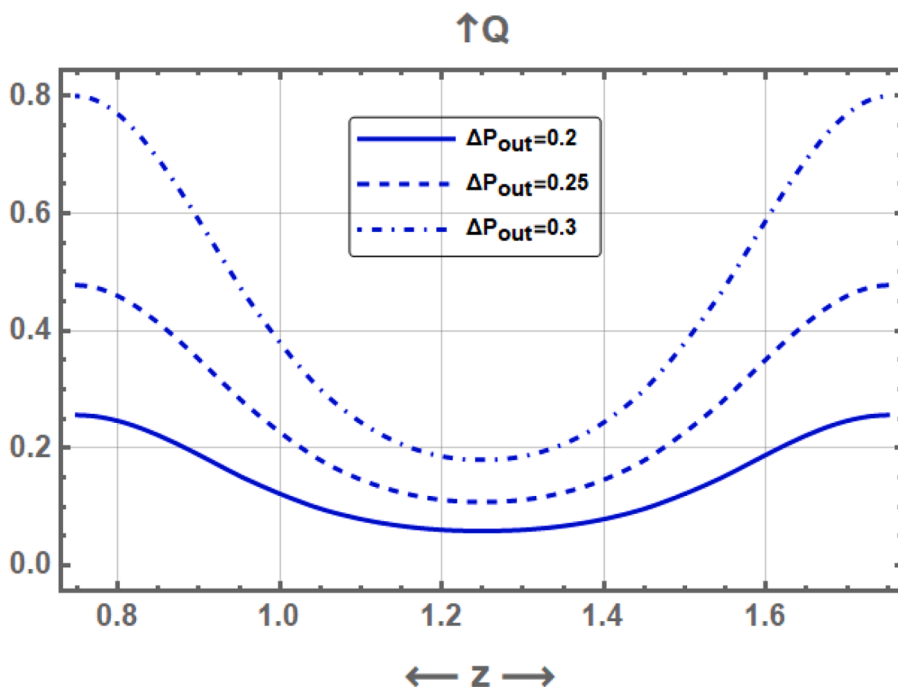


Figure 13. Mazumdar model (variation of flux  $Q$  with  $z$  for different values of  $\Delta P_{out}$ ).

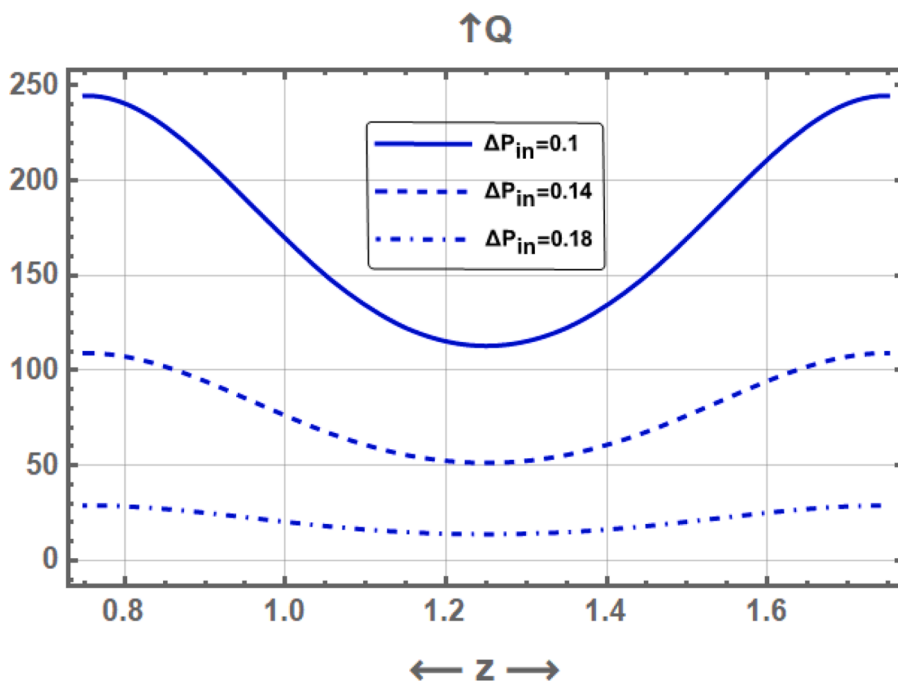


Figure 14. Keller model (variation of flux  $Q$  with  $z$  for different values of  $\Delta P_{in}$ ).

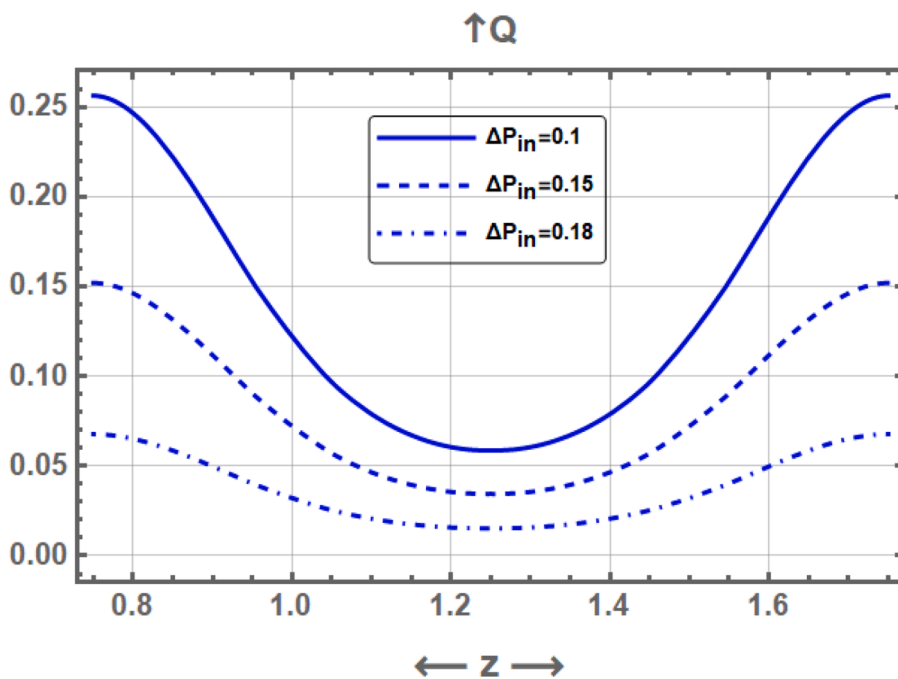


Figure 15. Mazumdar model (variation of flux  $Q$  with  $z$  for different values of  $\Delta P_{in}$ ).

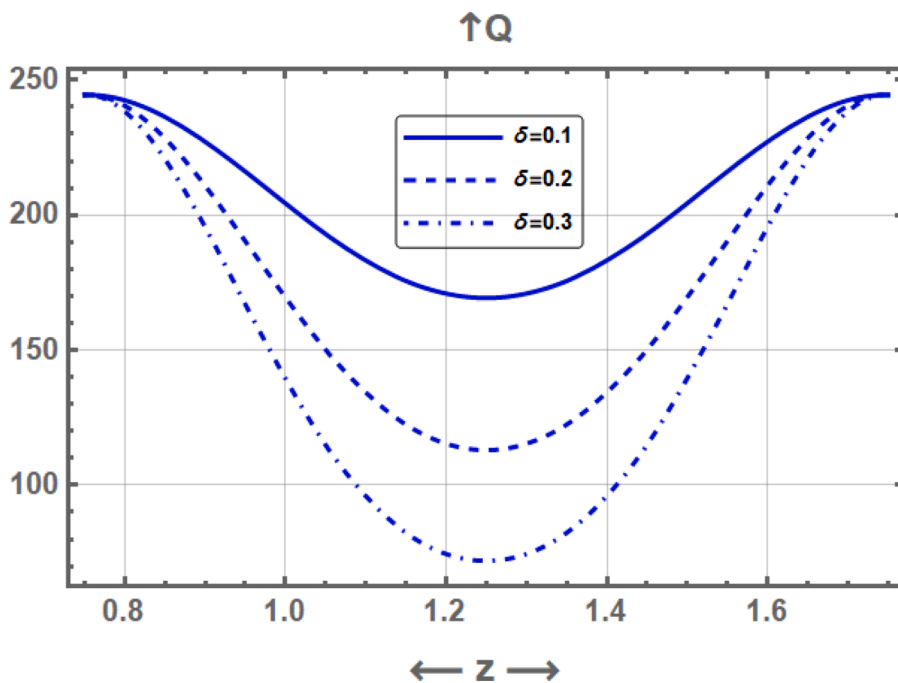


Figure 16. Keller model (variation of flux  $Q$  with  $z$  for different values of  $\delta$ ).

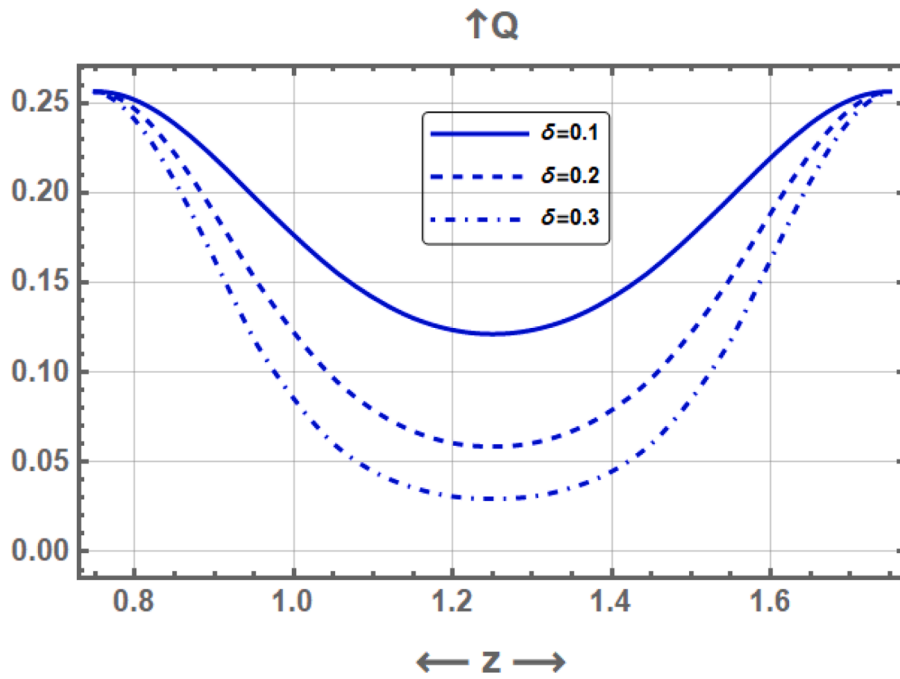


Figure 17. Mazumdar model (variation of flux  $Q$  with  $z$  for different values of  $\delta$ ).

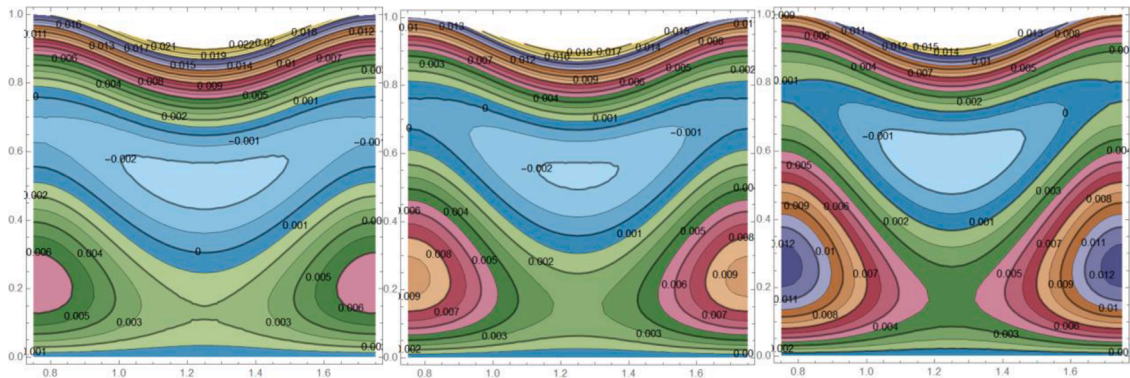


Figure 18. Stream line for (a)  $\tau_p = 0.1$ , (b)  $\tau_p = 0.11$ , (c)  $\tau_p = 0.12$ .

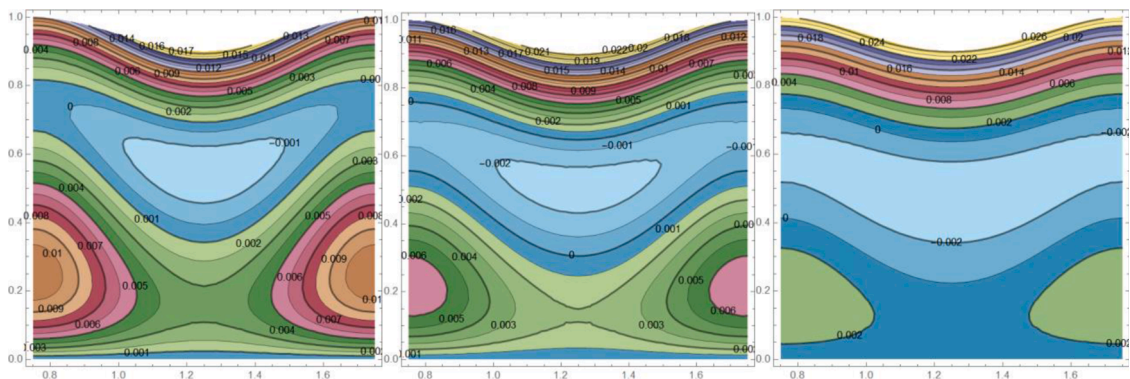


Figure 19. stream line for (a)  $\tau = 0$ , (b)  $\tau = 0.1$ , (c)  $\tau = 0.2$ .

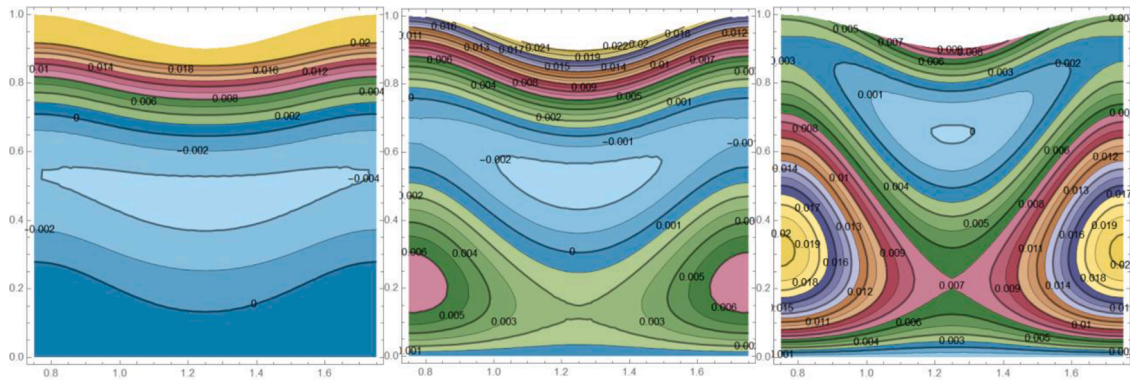


Figure 20. stream line for (a),  $R' = 0$  (b)  $R' = 0.1$ , (c)  $R' = 0.2$ .

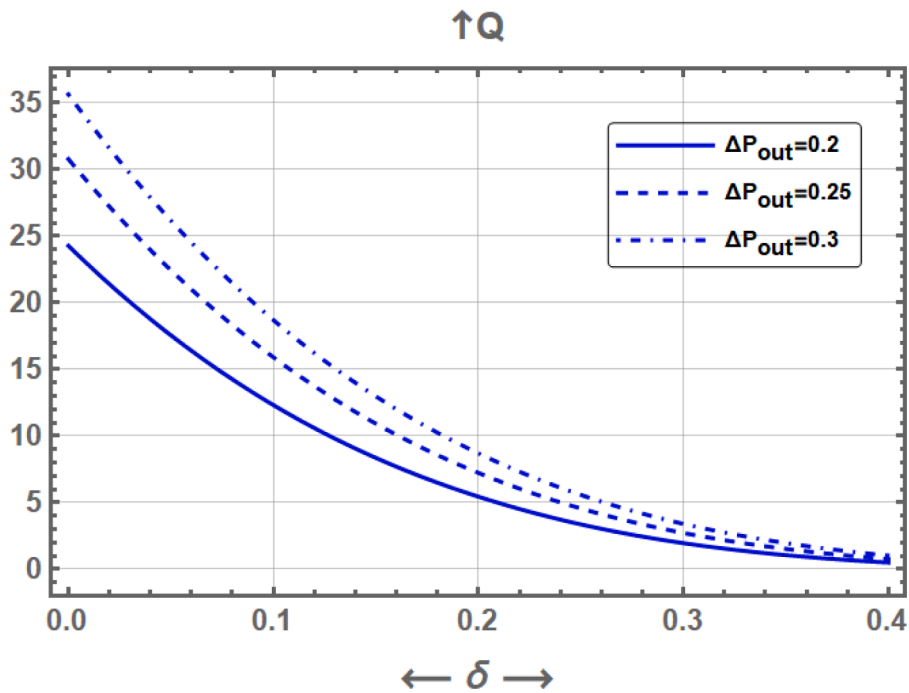


Figure 21. Keller model (variation of flux  $Q$  with  $\delta$  for different values of  $\Delta P_{out}$ ).

$$T(R') = A(e^{KR'} - e^K) \tag{32}$$

Where  $A = 0.007435$  and  $K = 5.2625$ . we substitute (32) in (28) we can obtain:

$$P' = P - P_0 = \frac{1}{R'} [A(e^{KR'} - e^K)] \tag{33}$$

$$dP' = A \left[ \frac{Ke^{KR'}}{R'} - \frac{e^{KR'} - e^K}{R'^2} \right] dR' \tag{34}$$

Using (34) in (27), we find that the flux as follows:

$$Q^n = AF^n \int_{P_2-P_0}^{P_1-P_0} (R + R')^{3n+1} \left[ \frac{Ke^{KR'}}{R'} - \frac{e^{KR'} - e^K}{R'^2} \right] dR'. \tag{35}$$

We can note that  $R$  and  $R'$  are identified through finding a solution to (28) with  $P = P_1$  and  $P_2$ , consequently. The previous integral (35) after numerical assessment, the flow value for Herschel-Bulkley’s model is given in an elastic tube. We observe that [equation \(35\)](#)

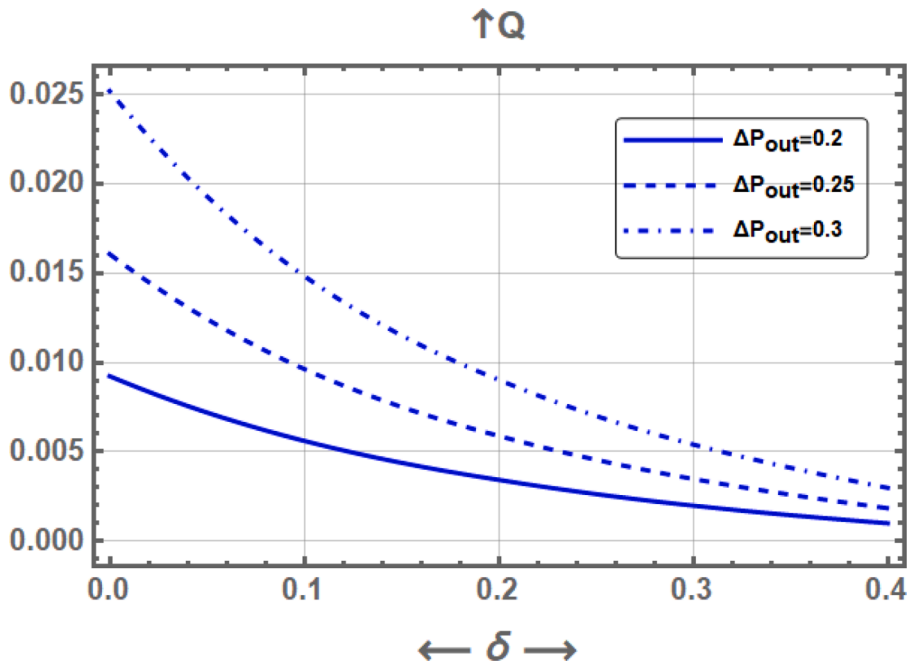


Figure 22. Mazumdar model (variation of flux  $Q$  with  $\delta$  for different values of  $\Delta P_{out}$ ).

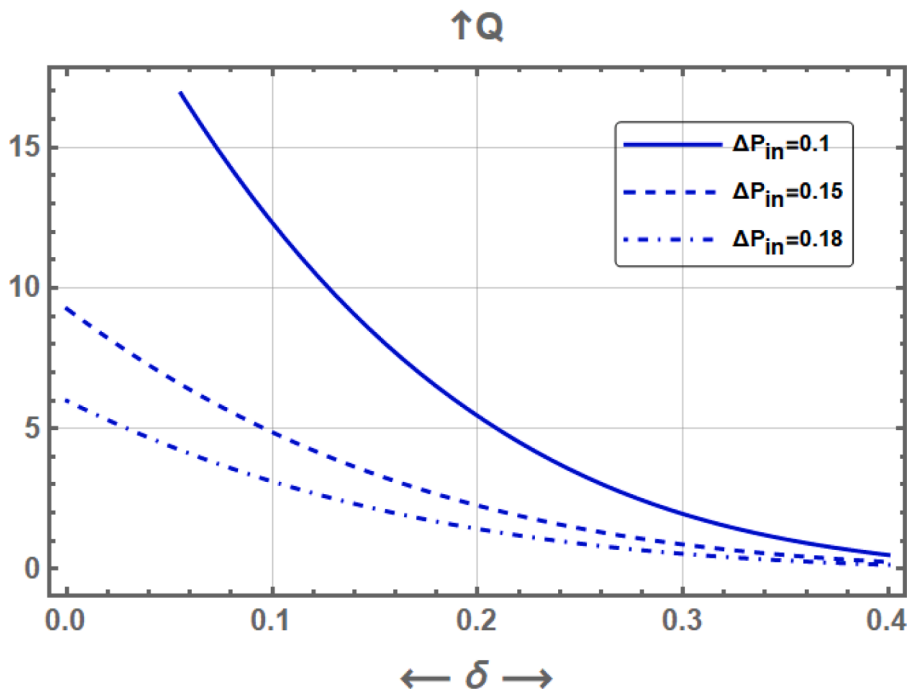


Figure 23. Keller model (variation of flux  $Q$  with  $\delta$  for different values of  $\Delta P_{in}$ ).

decreases to the matching consequences of Mazumdar [28] related to Herschel-Bulkley’s flow fluid in an elastic tube away from peristalsis (i.e.,  $R > 0$ ). Relying on the previous two phases, we find the Herschel-Bulkley fluid flow in an elastic tube.

#### 4. Validation

In this research paper, we work on the presence of a stenosis in the case of the elasticity of the walls. In order to clarify one of the

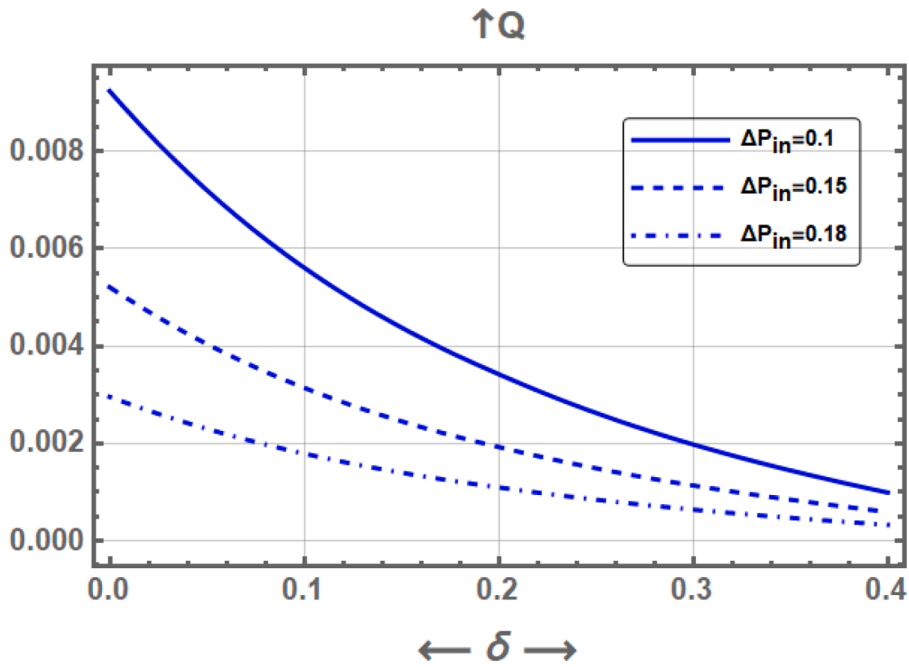


Figure 24. Mazumdar model (variation of flux  $Q$  with  $\delta$  for different values of  $\Delta P$ ).

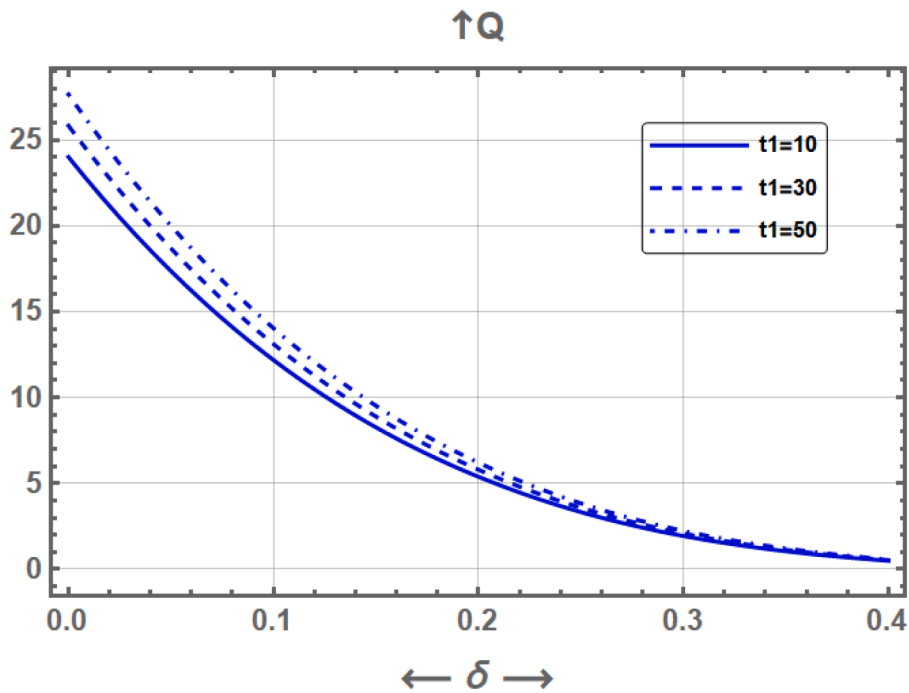


Figure 25. Keller model (variation of flux  $Q$  with  $\delta$  for different values of elastic parameter ( $t_1$ )).

differences, we substitute in the wall equation for  $\delta = 0$ , we extract the same results found in the research [22] as shown in table 1, and when we substitute by  $\delta$  with any value, we find (for example  $\delta = 0.1$ ) the results shown in table 1, and also the comparison between the results extracted by the Rubinow and Keller model [27], as well as the results extracted by the Mazumdar model [28].

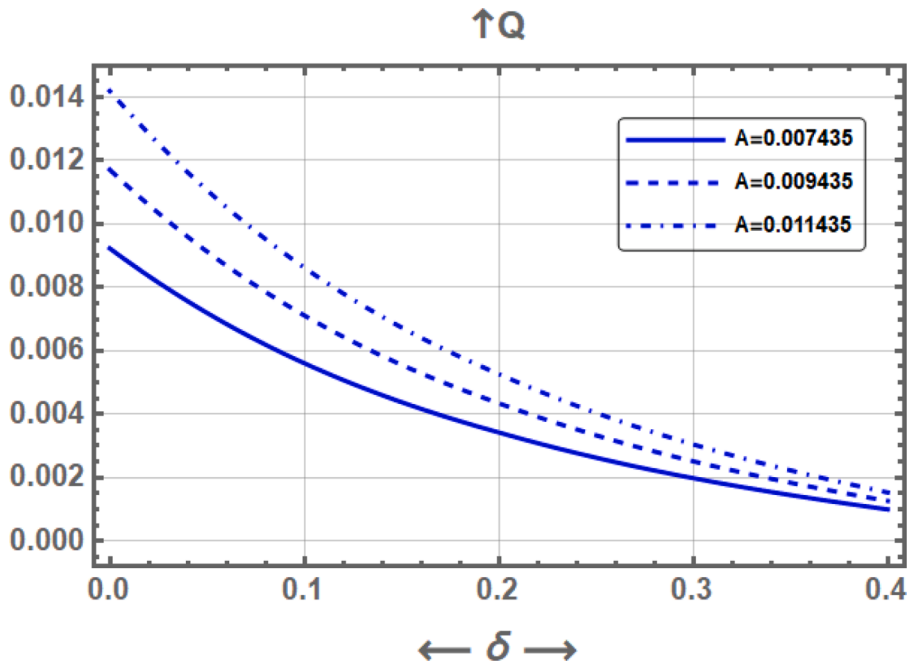


Figure 26. Mazumdar model (variation of flux  $Q$  with  $\delta$  for different values of elastic parameter ( $A$ )).

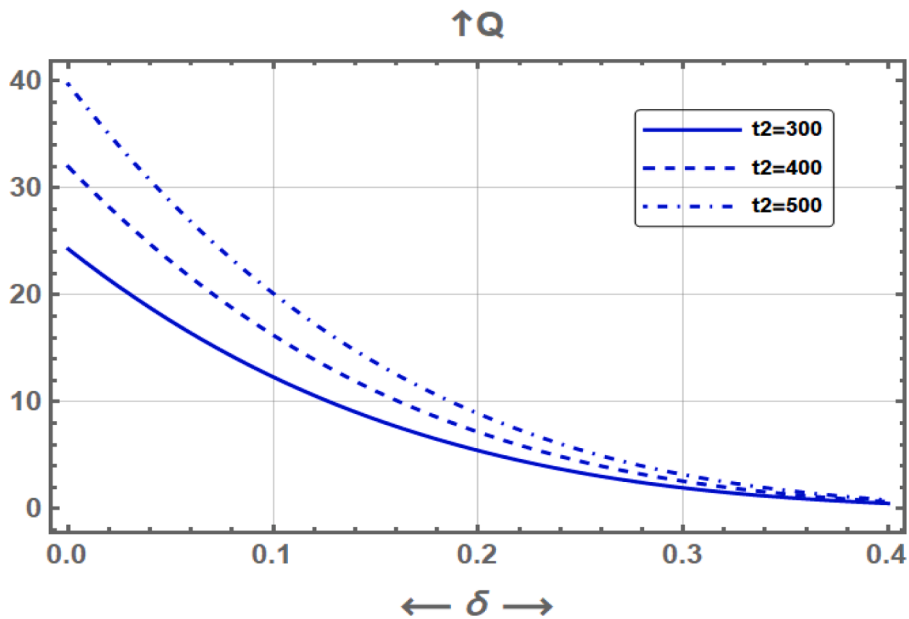


Figure 27. Keller model (variation of flux  $Q$  with  $\delta$  for different values of elastic parameter ( $t_2$ )).

### 5. Discussion and outcomes

This section divided in two subsections, flow rate with the tube axes ( $z$ ) and the flow rate with the highest stenosis ( $\delta$ ).

#### 5.1. Flow rate through the tube axis

The fundamental goal of this investigation is the alternation of the flow of blood in an elastic tube, as well as measuring the growth in the resistance of flow in a tiny artery due to the presence of blood stenosis and catheters, we can do that through modeling the blood of cows as fluid, Herschel-Bulkley. The fluid is assumed to be stable, laminar, fully developed, and axially symmetric. In this case, the

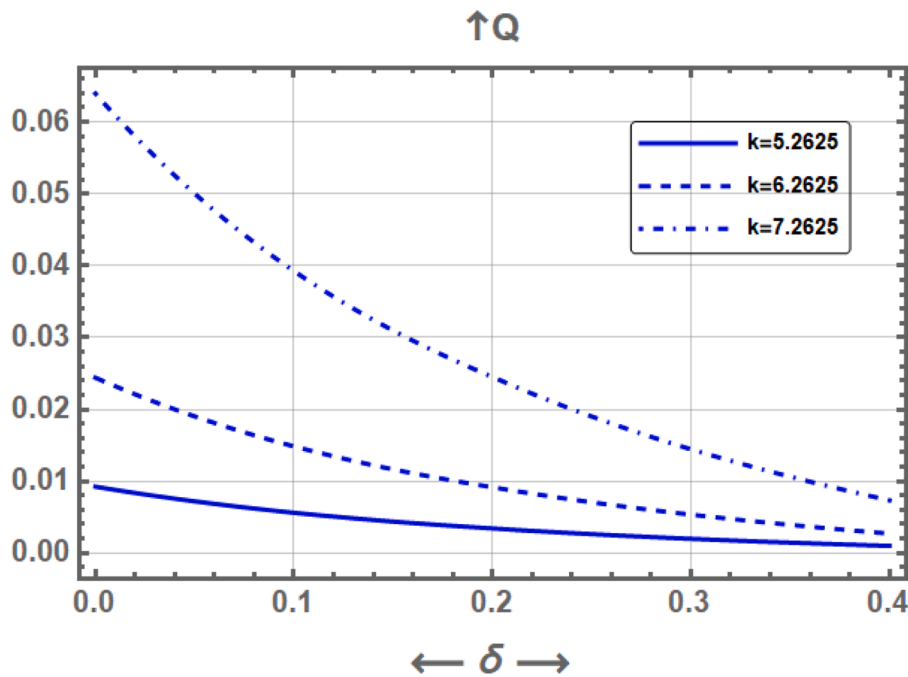


Figure 28. Mazumdar model (variation of flux  $Q$  with  $\delta$  for different values of other elastic parameter ( $k$ )).

blood is shaped as a Herschel-Bulkley fluid and that sample takes into consideration shear-stress formula, stenosis modulus and flexibility of wall. The current study also examines and analyzes the stenosis influences, catheter effects, non-Newtonian fluid, elastic tube features, flow, inner radius, outlet radius, and external pressures. The chief characteristic of this model is that it involves tension expressions as a multinomial function of the fifth degree as well as an elementary function as well as the power-law and Newtonian fluid models. So that we can make an evaluation to the quantitative consequences of the different formula included in the problem, we must perform numerical simulations/imitation by using the program "MATHEMATICA" of the outcome analytical expressions that are showed in Figures 2 to 20. Figure 2, declares that the flow rate  $Q$ , by the Rubinow and Keller method, is higher than the flow rate in the Bingham fluid and also higher than the fluid in the power-law and Herschel-Bulkley fluids. That is to say, in all cases the flow (Power-law, Herschel-Bulkley and Bingham) models is lower than that of Newtonian liquids. In addition, in Fig. 3 it is obvious that the flow  $Q$  using Mazumdar method in the Newtonian fluid's case is smoothly greater than the flow in the Bingham fluid, and this is somehow a little bit greater than the flow in the case of Herschel-Bulkley fluid as well as power-law fluid. In Fig. 4, the flow  $Q$ 's alternation is measured by the Rubinow and Keller method with the  $Z$  axis for various values of stress of shear; from the appeared figure, it is clear that the flow  $Q$  relies on the shear stress and reduces with increasing shear stress. Also, Fig 5 also shows the flow  $Q$  with the  $Z$  axis but in a Mazumdar method and shows also that the flow  $Q$  reduces with the increasing shear stress. Figures 6 and 7 declare the change of the flow  $Q$  with the  $Z$  axis with both methods: (Rubinow & Keller and Mazumdar) with the variation in power law-index ( $n$ ), which declares that the flow reduces with a growth in power law-index ( $n$ ), but to some extent, the flow also decreases by a little percentage. We also show the influences of varying the parameter of elastic  $t_1$  with the stability of the other parameters of elastic  $t_2$  through the Rubinow and Keller method and changing the parameter of elasticity  $A$  with the other parameter of elasticity  $K$  as related to the manner of Mazumdar. As noted in Figures 8 and 9 respectively, and as it appears that the flow in both cases increases with boosting the parameter of elasticity ( $t_1$  or  $A$ ). Besides, in Figures 10 and 11, the same previous consequence is produced by the variation in the parameter of flexibility, the variable is ( $t_2$  or  $K$ ) and the stable is ( $t_1$  or  $A$ ). That is to say, the flow increases with increasing in the modulus of elastic ( $t_2$  or  $K$ ). Looking at Figures 12 and 13 deeply, which show the flow  $Q$  with the  $Z$  axis by the two manners: Rubinow & Keller and Mazumdar respectively, with the difference in the outer pressure's variation from the external pressure, announces that there is an increase in the flow with the boost in the external pressure variation, which is different from the external pressure, as presented in the figure. In this case, the opposite takes place in Figures 14 and 15, as it is exposed that the flow  $Q$  decreases with the boost in the inner pressure's difference from the outlet pressure, and this is opposite to the outlet pressure's difference from the external pressure. On the contrary, Figures 16 and 17, illustrated by the different stenosis parameter, we can deduce that the more the stenosis coefficient increases, the more flow  $Q$  decreases. We also see from Figure 18, that with the increase in shear stress inside the catheter wall ( $\tau_p$ ), the streamlines increase and the number of bolus increases. We can also notice from Fig. 19, that bolus disappears with the growth in stress of yield ( $\tau$ ), and the fluid moves as a bulk. Finally, we find that from Figure 20, with the increase in the radius dilation ( $R'$ ), streamlines increase and bolus increases. These results are shown by both methods: Rubinow & Keller and Mazumdar.

## 5.2. Flow rate with the highest stenosis inside the artery

In Figures 21 and 22, we found that more  $\Delta P_{out}$  enhance the fluid flow. Also in case of Rubinow and Keller model the curves of  $Q$  are goes rapidly to vanish than that of Mazumdar model. On the contrary, in Figures 23 and 24, it is clear that an increase of  $\Delta p_{in}$  with  $\delta$ , the flow rate decreases for both models. From Figure 25, Figure 26, Figure 27, Figure 28, we found that the improvement in the elasticity coefficients ( $t_1$ ,  $t_2$ ,  $A$  and  $k$ ) for both models (Rubinow & Keller and Mazumdar) is followed by an improvement in the fluid flow, but for the elasticity coefficients ( $t_2$  and  $k$ ) there is a better flow rate for the fluid than other for the parameters elastic.

## 6. Conclusions

This study deals with the flow of a non-Newtonian fluid with non-zero yield stress, It's Herschel-Bulkley's fluid which aims at studying the variations in the flow of blood in case of inserting a catheter inside a flexible conduit in if there is a stenosis. The blood is designed to be considered as Herschel-Bulkley's fluid. This sample takes into consideration the shear stress, stenosis modulus and wall flexibility. The outcomes were examined for several values of the relevant parameters, radius, the stress of shear stability of tube wall and stenosis. Here is some of the most outstanding discoveries and findings:

- The flow raises with an increase in the tube's radius.
- The flow rate reduces with increasing values of the power-law index ( $n$ ) and the stress of yield ( $\tau$ ).
- The flow rate enhanced with more values of the wall flexible parameters.
- The inner and outer pressures have variable influences on the flow rate, and the flow rate increases with decreasing values of the stenosis parameter ( $\delta$ ).
- As related to the discussion and conclusions, The results showed that the increase in the parameters related to the elasticity of the walls enhanced blood flow through the stenosis area and also it is noted that the Rubinow and Keller manner is effective and more efficient than Mazumdar's model regarding the effect of shear stress, stenosis coefficient and power law-index.

## Declaration of Competing Interest

The authors declare that they have no known competing financial interests or personal relationships that could have appeared to influence the work reported in this paper.

## References

- [1] Kh.S. Mekheimer, M.A. Elkot, Mathematical modelling of unsteady flow of a Sisko fluid through an anisotropically tapered elastic arteries with time-variant overlapping stenosis, *Appl. Math. Model.* 36 (2012) 5393.
- [2] D.N. Riahi, R. Roy, S. Cavazos, On arterial blood flow in the overlapping stenosis, *Math. & Comp. Model.* 54 (2011) 2999.
- [3] S. Nadeem, S. Ijaz, Nanoparticles analysis on the blood flow through a tapered catheterized elastic artery with overlapping stenosis, *Eur. Phys. J. Plus* 129 (2014) 249.
- [4] Kh.S. Mekheimer, A.Z. Zaher, A.I. Abdellateef, Entropy hemodynamics particle-fluid suspension model through eccentric catheterization for time-variant stenotic arterial wall: Catheter injection, *International Journal of Geometric Methods in Modern Physics* 16 (2019), 1950164.
- [5] Kh.S. Mekheimer, Shahzadi Iqra, S. Nadeem, A.M.A. Moawad, A.Z. Zaher, Reactivity of bifurcation angle and electroosmosis flow for hemodynamic flow through aortic bifurcation and stenotic wall with heat transfer, *Phys. Scr.* 96 (2021), 015216.
- [6] Kh.S. Mekheimer, M.A. Elkot, Influence of Magnetic field and Hall currents on blood flow through stenotic artery, *Appl. Math. Mech. Eng. Ed.* 29 (2008) 1093.
- [7] S.I. Abdelsalam, Kh.S. Mekheimer, A.Z. Zaher, Alterations in blood stream by electroosmotic forces of hybrid nanofluid through diseased artery: Aneurysmal/stenosed segment, *Chinese Journal of Physics* 67 (2020) 314–329.
- [8] Y. Xu, J. Zhu, L. Zheng, et al., Non-Newtonian biomagnetic fluid flow through a stenosed bifurcated artery with a slip boundary condition, *Appl. Math. Mech.-Engl. Ed.* 41 (2020) 1611–1630.
- [9] ZHANG Xuelan, LUO Mingyao, TAN Peilai, ZHENG Liancun, SHU Chang, Magnetic nanoparticle drug targeting to patient-specific atherosclerosis: effects of magnetic field intensity and configuration, *Appl. Math. Mech.-Engl. Ed.* 41 (2) (2020) 349–360.
- [10] K. Vajravelu, S. Sreenadh, V. Ramesh-Babu, Peristaltic transport of a Herschel–Bulkley fluid in an inclined tube, *Int. J. Nonlin. Mech.* 40 (2005) 83.
- [11] S.R. Shah, R. Kumar, Mathematical Modeling of Blood Flow with the Suspension of Nanoparticles Through a Tapered Artery with a Blood Clot, *Front. Nanotechnol.*, *Front. Nanotechnol.* 2 (2020), 596475, <https://doi.org/10.3389/fnano.2020.596475>.
- [12] WU. Jie, CAI. Yan, FU. Yi, TAN Zhujun, SUN Ren, XU5. Shixiong, DING. Zurong, DONG. Cheng, 3D numerical study of tumor blood perfusion and oxygen transport during vascular normalization, *Appl. Math. Mech.-Engl. Ed.* 36 (2) (2015) 153–162.
- [13] R. Ellahi, S.U. Rahman, S. Nadeem, Blood flow of Jeffrey fluid in a catheterized tapered artery with the suspension of nanoparticles, *Physics Letters A* (2014) 2973–2980.
- [14] A. Mirza, M. Abdulhameed, S. Shafie, Magneto-hydrodynamic approach of non-Newtonian blood flow with magnetic particles in stenosed artery, *Appl. Math. Mech.-Engl. Ed.* 38 (3) (2017) 379–392.
- [15] M.M. Bhatti, A. Zeeshan, R. Ellahi, O. Anwar Bég, A. Kadir, Effects of coagulation on the two-phase peristaltic pumping of magnetized prandtl biofluid through an endoscopic annular geometry containing a porous medium, *Chinese Journal of Physics* 58 (2019) 222–234.
- [16] D. Tripathi, J. Prakash, R. Ellahi A.K. Tiwari, Thermal, microrotation, electromagnetic field and nanoparticle shape effects on Cu-CuO/blood flow in microvascular vessels, *Microvascular Research* 132 (2020), 104065, 2358.
- [17] S. Rana, R. Mehmood, M.M. Bhatti, Bioconvection oblique motion of magnetized Oldroyd-B fluid through an elastic surface with suction/injection, *Chinese Journal of Physics* 73 (2021) 314–330.
- [18] R. Ellahi, S.U.M. Rahman, M. Gulzar, S. Nadeem, K. Vafai, A Mathematical study of non-newtonian micropolar fluid in arterial blood flow through composite stenosis, *Appl. Math. Inf. Sci.* 8 (4) (2014) 1567–1573.
- [19] M.M. Bhatti, S.I. Abdelsalam, Bio-inspired peristaltic propulsion of hybrid nanofluid flow with Tantalum (Ta) and Gold (Au) nanoparticles under magnetic effects, *Waves in Random and Complex Media* 17455030 (2021), 1998728.
- [20] Asmaa F. Elelmy, Nasser S. Elgazery, R. Ellahi, Blood flow of MHD non-Newtonian nanofluid with heat transfer and slip effects: Application of bacterial growth in heart valve, *International Journal of Numerical Methods for Heat and Fluid Flow* 30 (11) (2020) 4883–4908.

- [21] H. Waqas, M. Imran, M.M. Bhatti, Influence of bioconvection on Maxwell nanofluid flow with the swimming of motile microorganisms over a vertical rotating cylinder, *Chinese Journal of Physics* 68 (2020) 558–577.
- [22] K. Vajravelu, S. Sreenadh, P. Devaki, K.V. Prasad, Mathematical model for a Herschel-Bulkley fluid flow in an elastic tube, *Central European Journal of Physics* 9 (5) (2011) 1357–1365.
- [23] T. Young, Hydraulic investigations, subservient to an intended croonian lecture on the motion of blood, *Phil. Trans. R. Soc. Lond.* 98 (1808) 164–186.
- [24] Y.C. Fung, *Biomechanics: Circulation*, 2nd edn, Springer Science business Media, New York, 1997.
- [25] T. Sochi, The flow of Newtonian and power law fluids in elastic tubes, *Int. J. Nonlinear Mech.* 67 (2014) 245–250.
- [26] M.R. Roach, A.C. Burton, The effect of age on the elasticity of human iliac arteries, *Can. J. Biochem. Phys.* 37 (1959) 557–570.
- [27] S.I. Rubinow, J.B. Keller, Flow of a viscous fluid through ad elastic tube with applications to blood flow, *J. Theor. Biol.* 35 (1972) 299.
- [28] N.J. Mazumdar, *Biofluid Mechanics*. World Scientific, Chap 5, 1992. Singapore.